Biomedical Optics EXPRESS

Geometry-invariant GRIN lens:
iso-dispersive contours

Mehdi Bahrami* **and Alexander V. Goncharov**
Applied Optics Group, National University of Ireland, Galway
Galway, Ireland
**m.bahrami1@nuigalway.ie*

Abstract: A dispersive model of a gradient refractive index (GRIN) lens is introduced based on the idea of iso-dispersive contours. These contours have constant Abbe number and their shape is related to iso-indicial contours of the monochromatic geometry-invariant GRIN lens (GIGL) model. The chromatic GIGL model predicts the dispersion throughout the GRIN structure by using the dispersion curves of the surface and the center of the lens. The analytical approach for paraxial ray tracing and the monochromatic aberration calculations used in the GIGL model is employed here to derive closed-form expressions for the axial and lateral color coefficients of the lens. Expressions for equivalent refractive index and the equivalent Abbe number of the homogeneous equivalent lens are also presented and new aspects of the chromatic aberration change due to aging are discussed. The key derivations and explanations of the GRIN lens optical properties are accompanied with numerical examples for the human and animal eye GRIN lenses.

© 2012 Optical Society of America

OCIS codes: (110.2760) Gradient-index lenses; (330.7326) Visual optics, modeling; (080.1005) Aberration expansions; (220.1000) Aberration compensation.

References and links

1. H. L. Liou and N. A. Brennan, "Anatomically accurate, finite model eye for optical modeling," J. Opt. Soc. Am. A **14,** 1684–1695 (1997).
2. J. A. Díaz, C. Pizarro, and J. Arasa, "Single dispersive gradient-index profile for the aging human lens," J. Opt. Soc. Am. A **25,** 250–261 (2008).
3. M. Bahrami and A. V. Goncharov, "Geometry-invariant GRIN lens: analytical ray tracing" J. Biomed. Opt. **17,** 055001 (2012).
4. B. K. Pierscionek, "Presbyopia - effect of refractive index," Clin. Exp. Optom. **73,** 23–30 (1990).
5. G. Smith, D. A. Atchison, and B. K. Pierscionek, "Modeling the power of the aging human eye," J. Opt. Soc. Am. A **9,** 2111–2117 (1992).
6. G. Smith and B. K. Pierscionek, "The optical structure of the lens and its contribution to the refractive status of the eye," Ophthalmic Physiol. Opt. **18,** 21–29 (1998).
7. C. E. Jones, D. A. Atchison, R. Meder, and J. M. Pope, "Refractive index distribution and optical properties of the isolated human lens measured using magnetic resonance imaging (MRI)," Vision Res. **45,** 2352–2366 (2005).
8. R. Navarro, F. Palos, and L. González, "Adaptive model of the gradient index of the human lens. I. formulation and model of aging ex vivo lenses," J. Opt. Soc. Am. A **24,** 2175–2185 (2007).
9. S. Kasthurirangan, E. L. Markwell, D. A. Atchison, and J. M. Pope, "In vivo study of changes in refractive index distribution in the human crystalline lens with age and accommodation," Invest. Ophthalmol. Vis. Sci. **49,** 2531–2540 (2008).
10. D. A. Palmer and J. Sivak, "Crystalline lens dispersion," J. Opt. Soc. Am. A **71,** 780–782 (1981).
11. J. G. Sivak and T. Mandelman, "Chromatic dispersion of the ocular media," Vision Res. **22,** 997–1003 (1982).
12. D. A. Atchison and G. Smith, "Chromatic dispersions of the ocular media of human eyes," J. Opt. Soc. Am. A **22,** 29–37 (2005).

13. The geometry-Invariant lens computational code. This is a computable document format (CDF) for the equations presented in Ref. [3]. Our source CDF code can be accessed via Mathematica, the computational software developed by Wolfram Research (Oct. 2011), *http://optics.nuigalway.ie/people/mehdiB/CDF.html*.

14. M. J. Kidger, *Fundamental Optical Design* (SPIE Press, 2002).

15. B. Gilmartin and R. E. Hogan, "The magnitude of longitudinal chromatic aberration of the human eye between 458 and 633 nm," Vision Res. **25,** 1747–1755 (1985).

16. R. I. Barraquer, R. Michael, R. Abreu, J. Lamarca, and F. Tresserra, "Human lens capsule thickness as a function of age and location along the sagittal lens perimeter," Invest. Ophthalmol. Vis. Sci. **47,** 2053–2060 (2006).

17. Y. Le Grand, *Form and Space Vision*, rev. ed., translated by M. Millodot and G. Heath (Indiana University Press, 1967).

18. R. Navarro, J. Santamaría, and J. Bescós, "Accommodation dependent model of the human eye with aspherics," J. Opt. Soc. Am. A **2,** 1273–1281 (1985).

19. S. R. Uhlhorn, D. Borja, F. Manns, and J. M. Parel, "Refractive index measurement of the isolated crystalline lens using optical coherence tomography," Vision Res. **48,** 2732–2738 (2008).

20. C. Ware, "Human axial chromatic aberration found not to decline with age," A. Graefes Arch. Klin. Exp. Ophthalmol. **218,** 39–41 (1982).

21. P. A. Howarth, X. X. Zhang, D. L. Still, and L. N. Thibos, "Does the chromatic aberration of the eye vary with age?," J. Opt. Soc. Am. A **5,** 2087–2096 (1988).

22. M. Millodot, "The influence of age on the chromatic aberration of the eye," A. Graefes Arch. Klin. Exp. Ophthalmol. **198,** 235–243 (1976).

23. J. A. Mordi and W. K. Adrian, "Influence of age on chromatic aberration of the human eye," A. Graefes Arch. Klin. Exp. Ophthalmol. **198,** 235–243 (1976).

24. N. Brown, "The change in lens curvature with age," Exp. Eye Res. **19,** 175–183 (1974).

25. A. V. Goncharov and C. Dainty, "Wide-field schematic eye models with gradient-index lens," J. Opt. Soc. Am. A **24,** 2157–2174 (2007).

26. R. H. H. Kröger and M. C. W. Campbell, "Dispersion and longitudinal chromatic aberration of the crystalline lens of the African cichlid fish Haplochromis burtoni," J. Opt. Soc. Am. A **13,** 2341–2347 (1996).

27. W. S. Jagger and P. J. Standsl, "A wide-angle gradient index optical model of the crystalline lens and eye of the octopus," Vision Res. **39,** 2841–2852 (1999).

1. Introduction

The experimental studies have shown a spatial change in chromatic dispersion of the gradient index (GRIN) eye lens. In spite of a noticeable variety in human GRIN lens models, modeling the dispersion of the GRIN lens has been considered only in two studies, [1] and [2]. However, the existing chromatic models of the GRIN lens do not have enough flexibility to be consistent with the experimental data that shows different amount of dispersion at the surface and the center of the GRIN lens. To understand the origin of chromatic effects in the GRIN lens and the corresponding aberrations arising from the spatial change of dispersion within the lens, one should consider the chromatic contribution of different layers in the GRIN structure. For doing this, we need at least to develop a paraxial ray tracing method (preferably analytical) for predicting the ray path within GRIN structure at different wavelengths. The paraxial ray-tracing will be the basis for calculating chromatic aberration of the GRIN structure, provided that the dispersion model for the surface and the center of the GRIN lens is given by experimental measurements.

In this paper we employ the geometry-invariant GRIN lens (GIGL) monochromatic model [3] and introduce wavelength dependence of the refractive index. This allows us to obtain a chromatic model matching experimental data on dispersion of the GRIN lens as well as to retain all properties of the GIGL mode including the analytical description for paraxial ray-tracing. Figure 1 depicts the GIGL geometry and its interior geometry-invariant iso-indicial contours, where R is the external radius of curvature and k is the external conic constant of the lens surfaces and subscripts 'a' and 'p' designate the anterior and the posterior surfaces, respectively, so that T_a and T_p are the axial thicknesses of the anterior and the posterior hemispheres, respectively. The sign convention used here is such that the radii and thicknesses are considered to be always positive as in our previous work [3]; however to be consistent with the
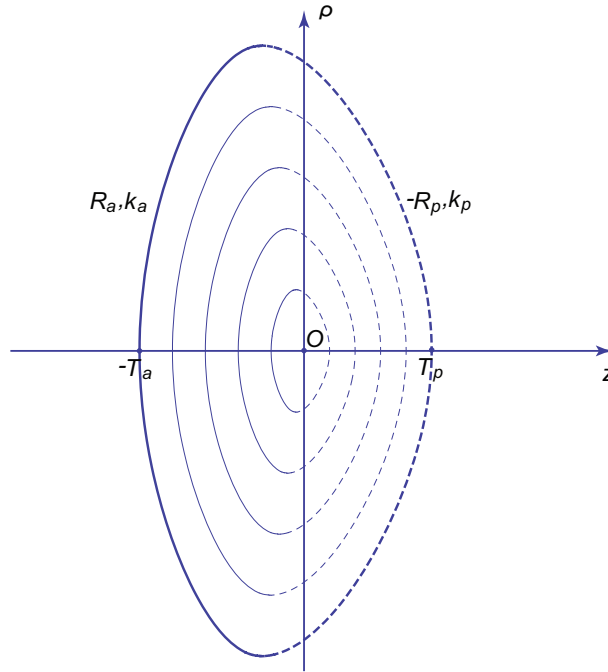
Fig. 1. The invariant-geometry GRIN lens and its interior iso-indicial contours [3].

optical design sign convention, we introduce '−' in front of T_a and R_p.

2. Dispersion model

2.1. Characteristics of dispersive GRIN lens

In the geometry-invariant GRIN lens model, the refractive index distribution is based on the power law profile, which was originally proposed by Pierscionek [4] and later supported by several studies [5–9]. In the GIGL model [3], this GRIN profile is presented as:

$$n(\zeta) = n_c + (n_s - n_c)(\zeta^2)^p;$$ (1)

where the parameter p in the exponent is employed to account for age-related dependence of the GRIN lens, ζ is the normalized distance from the center of the lens, and n_c and n_s are the refractive indices at the center and at the surface of the GRIN lens, respectively. Here, ζ varies between -1 to $+1$ to cover both anterior and posterior hemispheres of the lens. Note that the exponent p is not limited to integer numbers, so to avoid complex numbers we use the form $(\zeta^2)^p$. In monochromatic aberration studies, n_c and n_s are measured at a certain wavelength (typically at $\lambda_m = 555$ nm) for which the eye shows its highest sensitivity. It is well known that the GRIN lens is a dispersive medium with different dispersion characteristics at the center and at the surface [10, 11]. In other words, the GRIN refractive index profile is different at different wavelengths along the Z axis. We assume that these axial GRIN distribution profiles follow the power law with their own wavelength specific $n_c(\lambda)$, $n_s(\lambda)$ and $p(\lambda)$. In view of the well-known concept of iso-indicial contours in the GRIN lens, we propose the idea of iso-dispersive contours. We consider the lens structure consisting of very thin shells whit a constant chromatic dispersion (constant Abbe number). An iso-dispersive contour is the interface between the two adjacent shells.

There are several papers on suggesting theoretically sound equations for chromatic dispersion. Atchison *et al.* [12] have studied and reviewed experimental and theoretical data on ocular media dispersion and found the Cauchy's equation as the best fit:

$$n(\lambda) = A + \frac{B}{\lambda^2} + \frac{C}{\lambda^4} + \frac{D}{\lambda^6} + \ldots . \tag{2}$$

We use a modified representation of the Cauchy's equation as

$$n(\lambda) = n_m + n_{\lambda 2}\left(\frac{1}{\lambda^2} - \frac{1}{\lambda_m^2}\right) + n_{\lambda 4}\left(\frac{1}{\lambda^4} - \frac{1}{\lambda_m^4}\right), \tag{3}$$

where λ_m is the main wavelength and n_m is the refractive index at λ_m. n_m, $n_{\lambda 2}$ and $n_{\lambda 4}$ could be found by fitting Eq. (3) to a given dispersion data. Considering the experimental error in one of the dispersion measurements (Ref. [10]) used in the present paper, having only three terms in Eq. (3) provides an acceptable fit. In our experience, employing higher terms of Cauchy's equation gives the fitted curve a freedom to follow the noise in the data and even to develop a minimum, which does not correspond to a theoretically valid dispersion function.

Equation (1) can be rewritten to describe a dispersive GRIN medium as

$$n(\zeta, \lambda) = n_{center}(\lambda) + \left(n_{surface}(\lambda) - n_{center}(\lambda)\right)(\zeta^2)^{p(\lambda)}, \tag{4}$$

where

$$n_{center}(\lambda) = n_c + n_{c\lambda 2}\left(\frac{1}{\lambda^2} - \frac{1}{\lambda_m^2}\right) + n_{c\lambda 4}\left(\frac{1}{\lambda^4} - \frac{1}{\lambda_m^4}\right), \tag{5}$$

and

$$n_{surface}(\lambda) = n_s + n_{s\lambda 2}\left(\frac{1}{\lambda^2} - \frac{1}{\lambda_m^2}\right) + n_{s\lambda 4}\left(\frac{1}{\lambda^4} - \frac{1}{\lambda_m^4}\right). \tag{6}$$

n_c and n_s are respectively the refractive indices at the center and at the surface of the GRIN lens at the main wavelength λ_m, since Eq. (4) would be reduced to Eq. (1) where $\lambda = \lambda_m$. Therefore any characteristic of the lens (*e.g.* the optical power equations and the third-order aberration representations) defined for the monochromatic GIGL model [3, 13] will remain unchanged when using this representation.

To our knowledge this is the first attempt to represent the dispersive nature of the GRIN lens structure in terms of wavelength-dependent $n_{center}(\lambda)$, $n_{surface}(\lambda)$, and $p(\lambda)$. In the following section we show two numerical examples that emphasize the advantage of using this model when experimental dispersion data for the center and the surface of the lens is available.

2.2. Numerical examples

Equation (4) describes the gradual change in dispersion from the surface to the center of the lens. There are not so many published experimental data on the spatial change in dispersion of the GRIN lens in the human. These available data are limited to the dispersion curves at the center and the surface of the lens. This does not provide enough information to determine the rate of change in GRIN profile at any specific wavelength, which corresponds to the exponent $p(\lambda)$. Due to the lack of experimental data on wavelength dependence of the exponent $p(\lambda)$, for now, we limit our examples to the case of constant p. However the presented model is capable of taking into account the wavelength dependence of $p(\lambda)$ when more complete data become available. In the following, two sets of data are used to determine all the coefficients in the dispersive GRIN structure given by Eq. (4).

Palmer and Sivak [10] have done a series of measurements on a 70 year old eye for the wavelength range from 410 nm to 680 nm. It is worth mentioning that Palmer and Sivak have
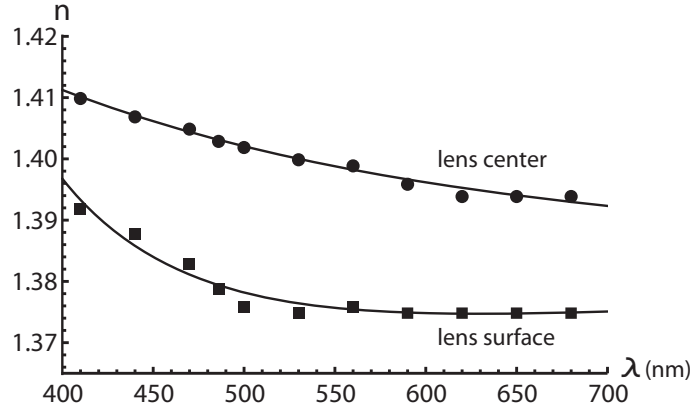
Fig. 2. The fit of the dispersion curves at the center and the surface of the lens to the dispersion data from Palmer and Sivak for a 70 year old eye [10].

stated that the material of the lens has not been altogether homogeneous and there have been inclusions of lower refractive index. Due to this, their data may not be as reliable as other data from human lenses. Figure 2 depicts their data and the least square fit using Eqs. (5) and (6). The fitting equations are

$$n_{center}(\lambda) = 1.39879 + 6241.59 \left(\frac{1}{\lambda^2} - \frac{1}{555^2} \right) - 2.10368 \times 10^8 \left(\frac{1}{\lambda^4} - \frac{1}{555^4} \right), \quad (7)$$

and

$$n_{surface}(\lambda) = 1.37555 - 7994.17 \left(\frac{1}{\lambda^2} - \frac{1}{555^2} \right) + 1.58549 \times 10^9 \left(\frac{1}{\lambda^4} - \frac{1}{555^4} \right). \quad (8)$$

In another work, Sivak and Mandelman [11] measured the GRIN lens dispersion of several subjects from 16-year old to 78-year old. They have provided averaged data for the dispersion curves of the center and the surface of the lens. Figure 3 shows the dispersion curves from the least square fit using Eqs. (5) and (6) to Sivak and Mandelman's data averaged over 6 to 9 separate eyes given by

$$n_{center}(\lambda) = 1.40395 + 7256.06 \left(\frac{1}{\lambda^2} - \frac{1}{555^2} \right) - 1.54846 \times 10^8 \left(\frac{1}{\lambda^4} - \frac{1}{555^4} \right), \quad (9)$$

and

$$n_{surface}(\lambda) = 1.37763 + 9260.03 \left(\frac{1}{\lambda^2} - \frac{1}{555^2} \right) - 3.12554 \times 10^8 \left(\frac{1}{\lambda^4} - \frac{1}{555^4} \right). \quad (10)$$

In addition to this, Fig. 4 demonstrates the dispersion curves across the lens provided by Eq. (4) for p equal to 2.0 and 5.0. This range is chosen in relation to the fitting results by Navarro *et al.* [8], where the case $p = 2.0$ could be considered as an extreme minimum for the refractive index profile of a very young healthy eye, whereas $p = 5.0$ corresponds to an aged eye. The intermediate curves between the lens center and surface show internal dispersion of the lens material predicted by Eq. (4) for ζ equal to 0.1, 0.2, ..., 0.9. The spacing between these curves indicates the power profile of the GRIN structure (characterized by exponent p).

Another way of distinguishing two cases ($p = 2.0$ and $p = 5.0$) is examining the refractive index profiles along the lens optical axis; these profiles are shown in Fig. 5. Figure 5 illustrates an age-related alteration originally suggested by Pierscionek [4] in the *lens paradox* explanation.
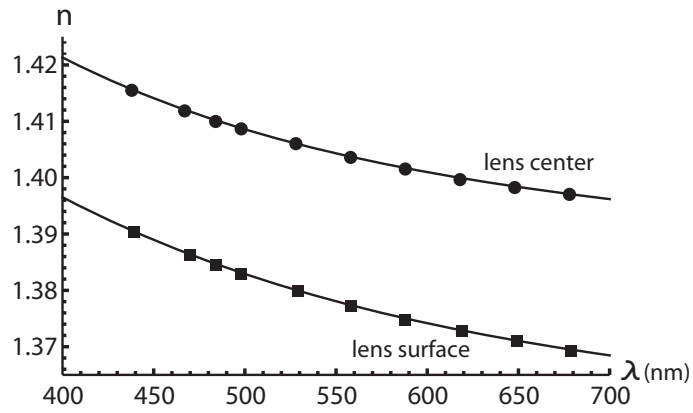
Fig. 3. The fit of the dispersion curves at the center and the surface of the lens to the dispersion data from Sivak and Mandelman [11].
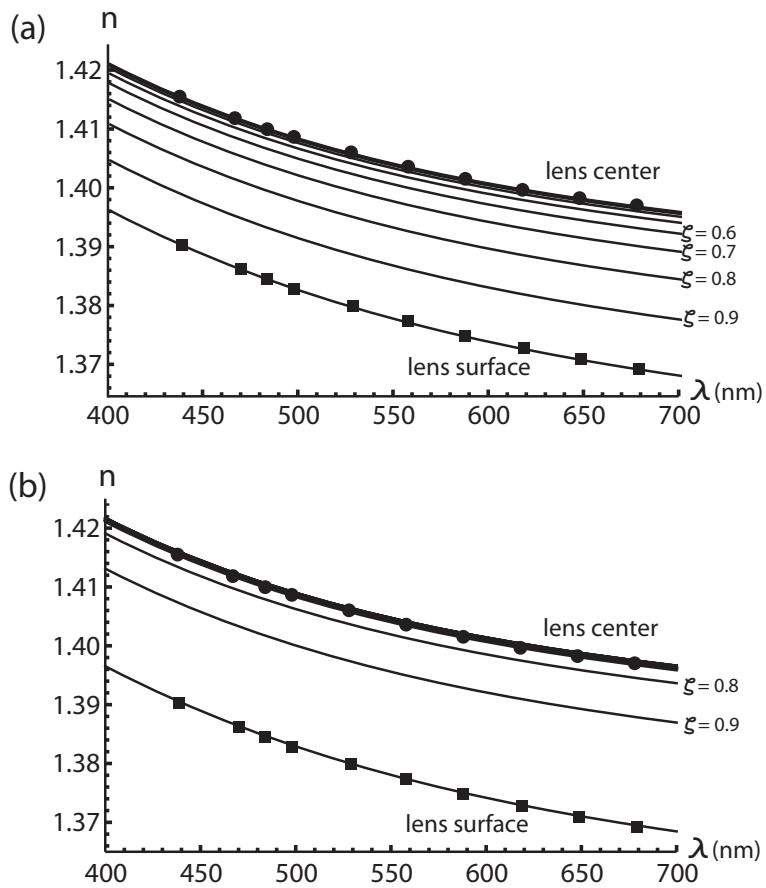

Fig. 4. The fit of the dispersion curves at the center and the surface of the lens to the dispersion data from Sivak and Mandelman [11], and our calculated dispersion curves across the lens employing Eq. (4) for (a) $p = 2.0$ and (b) $p = 5.0$.
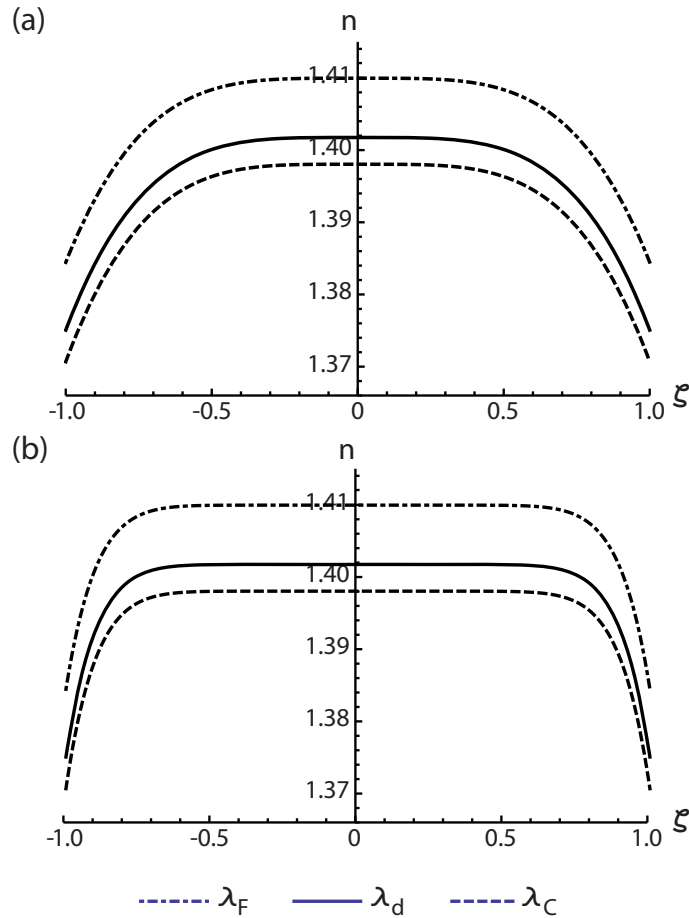
Fig. 5. The refractive index profiles across the lens for $\lambda_F = 486.1$ nm, $\lambda_d = 587.6$ nm, and $\lambda_C = 656.3$ nm using Eq. (4) for (a) $p = 2.0$ and (b) $p = 5.0$ fit to the dispersion data from Sivak and Mandelman [11].

3.   Chromatic aberration

3.1.   Chromatic coefficients

Using the idea of thin, iso-dispersive shells, we shall describe the chromatic effects occurring within the bulk of the lens. For this we need to revisit the definition of the axial and transverse chromatic aberrations in terms of paraxial optics.

The axial color coefficient for a single refractive surface C_L [14] is given by

$$C_L = n_d y \left(\frac{y}{r} + u \right) \left(\frac{n_d - 1}{n_d V_d} - \frac{n'_d - 1}{n'_d V'_d} \right), \tag{11}$$

where n_d is the refractive index of the medium at the spectral line d ($\lambda_d = 587.6$ nm) before the surface, y and u are the height and the angle of the incident ray at the surface, respectively, r is the surface radius of curvature, and V_d and V'_d are the Abbe numbers of the media respectively before and after the surface. The Abbe number is defined as

$$V_d = \frac{n_d - 1}{n_F - n_c}, \tag{12}$$

where n_F and n_c are the refractive indices of the medium at the spectral line F ($\lambda_F = 486.1$ nm) and the spectral line C ($\lambda_C = 656.3$ nm), respectively.

By adding the C_L coefficients of all surfaces in an optical system the total axial color coefficient is obtained. Using this coefficient, the axial distance between the image position at F and C wavelengths can be calculated as longitudinal axial chromatic aberration δ_{AX},

$$\delta_{AX} = \frac{1}{n_{di}u_i^2}C_L, \tag{13}$$

where n_{di} is the refractive index at d line in the last medium and u_i is the refracted ray angle at the image plane.

In a similar way, the lateral color coefficient C_T is given by

$$C_T = n_d y \left(\frac{y_c}{r} + u_c \right) \left(\frac{n_d - 1}{n_d V_d} - \frac{n'_d - 1}{n'_d V'_d} \right), \tag{14}$$

where y_c and u_c are the height and the angle of the incident chief (principal) ray at a refractive surface, respectively. The total coefficient C_T can be used in calculating the transverse lateral chromatic aberration δ_{TLC}, which corresponds to the vertical distance between the images at F and C wavelengths:

$$\delta_{TLC} = \frac{1}{n_{di}u_i}C_T. \tag{15}$$

The total axial and lateral color coefficients of a GRIN lens are the key to understanding its chromatic behavior in the eye. Using the paraxial ray tracing as in our derivation of the monochromatic aberrations in the GIGL model [3], the total chromatic coefficients can be obtained for the dispersive GRIN structure. Following the analytical ray tracing through the GIGL model, we shall derive the expressions for the axial and lateral color coefficients. First we define the Abbe number of the iso-dispersive shells Using Eq. (4)

$$V_d(\zeta) = \frac{n(\zeta, \lambda_d) - 1}{n(\zeta, \lambda_F) - n(\zeta, \lambda_C)}, \tag{16}$$

In general ζ corresponds to the normalized distance from the lens center to any point in the lens. The distance ζ along the optical axis is simply z/T_a and z/T_p for the anterior and posterior hemispheres, respectively. For a constant Abbe number V_d Eq. (16) defines the corresponding constant ζ of the iso-dispersive contour.

Equation (16) can be described in terms of axial distance z for paraxial ray tracing. Employing Eqs. (11), (4), and (16) we find the contribution of a thin layer with the thickness of δz within the GRIN structure in the total axial color coefficient of the lens as

$$\delta C_L = n \left(\frac{z}{T}, \lambda_d \right) y(z) \left(\frac{y(z)}{-Rz} + \frac{y'(z)}{T} \right) \left[\frac{\partial n}{\partial z} \left(\frac{z}{T}, \lambda_d \right) \left(n \left(\frac{z}{T}, \lambda_F \right) - n \left(\frac{z}{T}, \lambda_C \right) \right) - \right.$$
$$\left. - n \left(\frac{z}{T}, \lambda_d \right) \left(\frac{\partial n}{\partial z} \left(\frac{z}{T}, \lambda_F \right) - \frac{\partial n}{\partial z} \left(\frac{z}{T}, \lambda_C \right) \right) \right] / n^2 \left(\frac{z}{T}, \lambda_d \right) \delta z, \tag{17}$$

where $y(z)$ is the height of the ray inside the GRIN lens and R is the radius of curvature of the surface; the analytical expression for $y(z)$ in the GIGL model is derived in Ref. [3]. By summing up the contributions from all infinitely thin layers in the GRIN structure (where R equals to R_a and R_p in the anterior and posterior hemispheres, respectively) and including the contributions from the external surfaces of the lens we find the total axial color coefficient of

the lens,

$$\sum C_L = n_{aqu} y_0 \left(\frac{y_0}{R_a} + u_a \right) \left(\frac{n_{aqu} - 1}{n_{aqu} V_{aqu}} - \frac{n(-1, \lambda_d) - 1}{n(-1, \lambda_d) V_d(-1)} \right) +$$
$$+ \int_{-T_a}^{T_p} dC_L + n(1, \lambda_d) y(T_p) \left(\frac{y(T_p)}{-R_p} + u(T_p) \right) \left(\frac{n(1, \lambda_d) - 1}{n(1, \lambda_d) V_d(1)} - \frac{n_{vit} - 1}{n_{vit} V_{vit}} \right), \quad (18)$$

where y_0 and u_a are respectively the height and angle of the marginal ray at the anterior surface, $y(T_p)$ and $u(T_p)$ are respectively the height and the angle of the marginal ray just before the posterior surface, n_{aqu} and V_{aqu} are respectively the refractive index and the Abbe number of the medium before the lens at the d line, and n_{vit} and V_{vit} correspond to the medium after the lens. It is worth noticing that the ray tracing for these calculations should be done at the d line.

Similarly the coefficients for the lateral color of the lens is given by

$$\delta C_T = n \left(\frac{z}{T}, \lambda_d \right) y(z) \left(\frac{y_c(z)}{-Rz} + \frac{y_c'(z)}{T} \right) \left[\frac{\partial n}{\partial z} \left(\frac{z}{T}, \lambda_d \right) \left(n \left(\frac{z}{T}, \lambda_F \right) - n \left(\frac{z}{T}, \lambda_C \right) \right) - \right.$$
$$\left. - n \left(\frac{z}{T}, \lambda_d \right) \left(\frac{\partial n}{\partial z} \left(\frac{z}{T}, \lambda_F \right) - \frac{\partial n}{\partial z} \left(\frac{z}{T}, \lambda_C \right) \right) \right] / n^2 \left(\frac{z}{T}, \lambda_d \right) \delta z, \quad (19)$$

where $y_c(z)$ is the chief ray height inside the lens. Assuming the aperture stop is located at the anterior surface of the lens we obtain the total lateral color coefficient of the lens

$$\sum C_T = n_{aqu} y_0 u_{ca} \left(\frac{n_{aqu} - 1}{n_{aqu} V_{aqu}} - \frac{n(-1, \lambda_d) - 1}{n(-1, \lambda_d) V_d(-1)} \right) +$$
$$+ \int_{-T_a}^{T_p} dC_T + n(1, \lambda_d) y(T_p) \left(\frac{y_c(T_p)}{-R_p} + u_c(T_p) \right) \left(\frac{n(1, \lambda_d) - 1}{n(1, \lambda_d) V_d(1)} - \frac{n_{vit} - 1}{n_{vit} V_{vit}} \right), \quad (20)$$

where u_{ca} is the angle of the chief ray at the anterior surface, and $y_c(T_p)$ and $u_c(T_p)$ are respectively the height and the angle of the chief ray just before the posterior surface of the lens.

At this stage we have all equations ready for analysis of chromatic effects in the GRIN lens.

3.2. Numerical example

Using Eqs. (18) and (20) we can calculate the chromatic effects arising from a typical GRIN lens. To use these two equations, one needs the dispersion data for the GRIN lens as well as the dispersion data for the medium surrounding the lens. For the media before and after the lens, the aqueous and vitreous, respectively, we have used combined data provided by Atchison and Smith in terms of coefficients for Cauchy equation presented in Table 5 in Ref. [12].

3.2.1. Sivak and Mandelman's experimental data

As an example, Table 1 presents a typical GRIN lens geometry and its surrounding media with dispersive characteristics. Since the eye GRIN lens receives a converging beam we shall take into account its convergence by assuming a typical corneal shape with the anterior and posterior radii of curvature of 7.8 mm and 6.7 mm, respectively, the corneal thickness of 0.5 mm, and the 3.5 mm axial distance to the GRIN lens. This corresponds to the marginal ray angle $u_a = -0.036352$ rad at the pupil such that $y_0 = 1$ mm. The aperture stop (iris) is located just before the anterior surface of the lens, so the height of the chief ray at the anterior surface of the lens is zero. For the object located at infinity and the full field of view of 2 deg the chief ray angle at the anterior surface of the lens is $u_{ca} = 0.015000$ rad.

Table 2 presents the chromatic coefficients of this typical GRIN lens for each part of the lens using the dispersion data from Sivak and Mandelman [11] in Eqs. (9) and (10). Here to describe

the dispersive GRIN medium in accordance with Eq. (11) we assumed $p = 4.0$, which impacts the magnitude of the coefficients C_L and C_T for the GRIN structure.

Axial color coefficients in Table 2 show an interesting compensation effect in axial chromatic aberration of the lens. The negative C_L arising from the peripheral surfaces is to some extent corrected by the positive C_L originating from the GRIN structure of the lens. To understand the origin of the sign in coefficient C_L we revisit Eq. (11). Assuming $u \ll y/r$ and noting that $0 < y$, it is clear that the radius of curvature r and the variation of the quantity $(n_d - 1)/(n_d V_d)$ play the main role in establishing the sign of the axial color coefficient.

Figure 6 illustrates the variation of the quantity $(n_d - 1)/(n_d V_d)$ inside the lens is positive for the anterior hemisphere and negative for the posterior hemisphere. On the other hand, the radius of curvature r for the iso-indicial contours in the GRIN structure is also positive in the anterior and negative in the posterior hemispheres, thus the overall sign of the axial color coefficient of the GRIN structure is positive in both hemispheres.

In contrast, the quantity $(n_d - 1)/(n_d V_d)$ in the medium before and after the lens (0.004979 and 0.004888 respectively) is less than that of the surface of the lens (0.010015). This leads to the negative axial color coefficients at both anterior and posterior lens surfaces, see Table 2. A similar approach could be used to understand the change of sign in lateral color coefficients of the lens, although for the posterior surface we have an additional contribution to the coefficient from the non-zero height of the chief ray.

Table 1. A typical GRIN lens geometry and the dispersive characteristics of the surrounding media at the d line. (*using Table 5 in Ref. [12].)

Lens geometry (mm)		Surrounding medium*	
T_a	2.10	n_{aqu}	1.3347
T_p	1.40	V_{aqu}	50.37
R_a	11.00	n_{vit}	1.3347
R_p	7.50	V_{vit}	51.30

Table 2. The chromatic coefficients of a typical GRIN lens defined in Table 1 with the dispersion data from Sivak and Mandelman [11] described by Eqs. (9) and (10).

Axial color coefficients	
C_L from the anterior surface	-0.000367
C_L from the GRIN structure	+0.000450
C_L from the posterior surface	-0.000958
$\sum C_L$	-0.000875
Lateral color coefficients	
C_T from the anterior surface	-0.000101
C_T from the GRIN structure	+0.000018
C_T from the posterior surface	+0.000047
$\sum C_T$	-0.000036

To get a feeling about the magnitude of calculated axial color coefficient, we also calculate the axial chromatic aberration δ_{AX} in the whole eye using this typical lens. We assume that the lens in the eye is not tilted and then the total axial color coefficient of the eye is the sum of the axial color coefficients of the cornea and the GRIN lens. We assume that the optical power of an average eye is 60 D and the corneal refractive index and Abbe number are $n_d = 1.3677$ and $V_d = 55.48$ [12], which corresponds to the axial color coefficient of -0.000843 for the cornea.
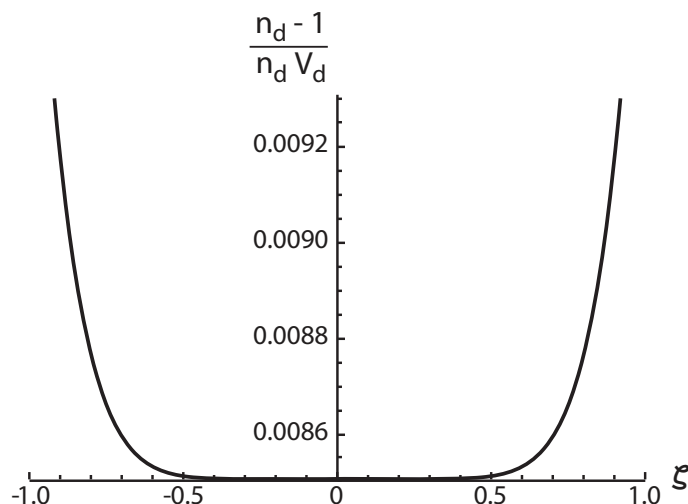
Fig. 6. The quantity $(n_d - 1)/(n_d V_d)$ as a function of ζ (the normalized distance from the lens center) using the dispersion data from Sivak and Mandelman [11] for $p = 4.0$.

The sum of the axial coefficients of the cornea and the lens is -0.001718, and from Eq. (13) we find that the axial chromatic aberration of this eye is 2.09 D. This amount of chromatic aberration is within the expected range of 1.87 ± 0.26 D found in the study by Gilmartin and Hogan [15], which used a similar spectral range of 488 nm and 633 nm.

In addition to the lens dispersion data, Sivak and Mandelman have also provided the dispersion of the capsule of the lens. To study the effect of the lens capsule dispersion on the lens axial color coefficient we have performed a numerical fit to Sivak and Mandelmans measurements using Eq. (3) for the capsule

$$n_{capsule}(\lambda) = 1.37108 + 2617.71 \left(\frac{1}{\lambda^2} - \frac{1}{555^2} \right) + 2.5783 \times 10^8 \left(\frac{1}{\lambda^4} - \frac{1}{555^4} \right). \qquad (21)$$

Table 3 provides the lens axial color coefficients using Eq. (21) and (11), which takes into account the chromatic effect of the lens capsule. For the anterior and the posterior layers of the lens capsule we have assumed a typical axial thickness of 0.015 mm and 0.002 mm, respectively [16]. A comparison of Tables 2 and 3 shows that the effect of the capsule is only

Table 3. The chromatic coefficients of a typical GRIN lens defined in Table 1 with the dispersion data from Sivak and Mandelman [11] on the eye lens capsule described by Eq. (21).

Axial color coefficients	
C_L from the anterior surface of the capsule	-0.000075
C_L from the anterior surface of the lens	-0.000292
C_L from the GRIN structure	+0.000450
C_L from the posterior surface of the lens	-0.000749
C_L from the posterior surface of the capsule	-0.000208
$\sum C_L$	-0.000874

0.1 percent of the total axial color coefficient and thus can be ignored. A closer look at Tables 2 and 3 reveals that the lens capsule does not change the magnitude of the chromatic effect
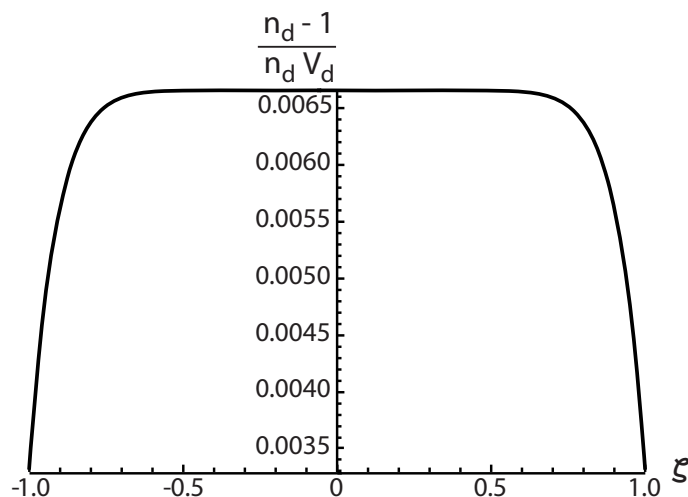
$$\frac{n_d - 1}{n_d V_d}$$

Fig. 7. The quantity $(n_d - 1)/(n_d V_d)$ as a function of ζ (the normalized distance from the lens center) using the dispersion data from Palmer and Sivak [10] for $p = 5.5$.

at the anterior and posterior surfaces of the lens. This is due to a very small thickness of the capsule, which means the radii of curvature of the capsule is very close to those of the lens, leading to a cancellation effect of the capsule contribution to the axial color coefficients.

3.2.2. Palmer and Sivak's experimental data

Employing the same lens geometry and the same dispersive characteristics of the surrounding media, we shall calculate the axial color coefficients of the lens using the dispersion data from the study by Palmer and Sivak of a 70 year old eye [10]. In this study the age of the eye is well defined, so we consider the exponent $p = 5.5$ based on the equation suggested by Navarro *et al.* [8] for connecting the exponent p to the age of the eye. Table 4 presents the color coefficients of the lens and Fig. 7 depicts the quantity $(n_d - 1)/(n_d V_d)$ as a function of the normalized distance ζ from the lens center.

Table 4. The chromatic coefficients of a typical GRIN lens defined in Table 1 with the dispersion data from Palmer and Sivak [10] described by Eqs. (7) and (8).

Axial color coefficients	
C_L from the anterior surface	+0.000120
C_L from the GRIN structure	-0.000948
C_L from the posterior surface	+0.000290
$\sum C_L$	-0.000537
Lateral color coefficients	
C_T from the anterior surface	+0.000033
C_T from the GRIN structure	-0.000038
C_T from the posterior surface	-0.000014
$\sum C_T$	-0.000019

In this example we can also see the compensation of chromatic aberrations in the lens, however in comparison to Table 2 the compensation happens in a different way. Table 4 indicates

that the GRIN structure of the lens produces a negative axial color coefficient, while the axial color coefficients of the external surfaces are positive. This is due to the different rate of growth of the quantity $(n_d - 1)/(n_d V_d)$ presented in Fig. 7, and also due to the different amount of the quantity $(n_d - 1)/(n_d V_d)$ at the lens surface, 0.003328, which is less than the surrounding media. As a result, the total axial color coefficient of the lens is still negative (-0.000537) in comparison with Table 2, but its absolute value is reduced by 20%. Using the same characteristics for the cornea, as in Section 3.2.1, the chromatic aberration of the whole eye becomes 1.68 D. This amount of chromatic aberration is within the expected range of 1.87 ± 0.26 D found in the study by Gilmartin and Hogan [15] using a similar spectral range.

3.2.3. Theoretical equations

In addition to the experimental data used in our two examples, it is worth revisiting the lens dispersion equations suggested by Atchison and Smith (Table 5 in Ref. [12]), which is based on the combined theoretical data from Le Grand [17] and Navarro *et al.* [18]. One can notice that the two equations describing the center and the surface dispersion can be reduced to the simple expression $n_{center}(\lambda) \simeq n_{surface}(\lambda) \times 1.014430$. For such a simple connection between the center and the surface dispersion curves, the quantity $(n_d - 1)/(n_d V_d)$ becomes independent of ζ terms and remains constant (0.006127) inside the GRIN lens. This becomes clear when we rewrite the quantity $(n_d - 1)/(n_d V_d)$ as $(n_F - n_c)/n_d$. The significance of the constancy of the quantity $(n_d - 1)/(n_d V_d)$ is that the GRIN structure is free from both chromatic effects (axial and lateral color) and only the external surfaces of the lens contribute to the chromatic aberrations. Table 5 shows this fact numerically under the same conditions considered in Table 1.

We would like to emphasize that for a non-dispersive GRIN structure as well as for a homogeneous refractive index lens (featuring in Le Grand [17] and Navarro *et al.* [18] models) one has only to worry about the dispersion description of the external surfaces of the lens. However the experimental data [10, 11] suggest that the chromatic contribution of the GRIN structure is comparable to that of the external surfaces, and furthermore plays an important role in the chromatic aberration compensation of the whole eye.

Table 5. The chromatic coefficients of a typical GRIN lens defined by Table 1 using the dispersion data from Atchison and Smith (Table 5 in Ref. [12]).

Axial color coefficients	
C_L from the anterior surface	-0.000084
C_L from the GRIN structure	+0.000000
C_L from the posterior surface	-0.000232
$\sum C_L$	-0.000315
Lateral color coefficients	
C_T from the anterior surface	-0.000023
C_T from the GRIN structure	+0.000000
C_T from the posterior surface	+0.000011
$\sum C_T$	-0.000012

It is worth mentioning that for achieving an achromatic lens (*i.e.* $\sum C_L = 0$), the axial color of the external surfaces is to be compensated by that from the GRIN structure, so the latter should not be zero. As an example of such aberration balancing, the lens in Section 3.2 can be made achromatic simply by adjusting one of the center dispersion coefficients, $n_{c\lambda 2}$, in Eq. (9) from 7256.06 to 5098.80. This corresponds to the change in the Abbe number of the lens center from 33.71 to 51.51, using Eq. (4). The example illustrates that the proposed dispersion model can

also help in developing bio-inspired lens designs, where the achromatic correction in individual components is needed.

4. Equivalent Abbe number approximation

It is a common practice, in the reduced eye models, to replace the GRIN lens by a simple lens providing spatially constant refractive index and Abbe number. Typically the characteristics of the eye lens in the reduced eye models are defined based on the optical power and axial chromatic aberration of the whole eye. In this section a different approach is proposed to calculate the equivalent Abbe number of the lens just using the experimental dispersion curves of the surface layer (cortex) and the center (core) of the GRIN lens. This approach may help in improving the reconstruction methods of a subject-specific GRIN lens.

The GIGL model provides a convenient equation for the optical power of the lens derived from a thin lens approximation as

$$F_{thin} = \frac{n_s - n_{aqu}}{R_a} + \frac{2p}{2p-1}(n_c - n_s)\left(\frac{1}{R_a} + \frac{1}{R_p}\right) + \frac{n_{vit} - n_s}{-R_p}. \tag{22}$$

For the crystalline lens Eq. (22) gives less than 1.4% error compared with the exact power calculations, and then can be a useful tool in the ocular calculations. The equivalent optical power of the lens defined as

$$F_{eqv} = \frac{n_{eqv} - n_{aqu}}{R_a} + \frac{n_{vit} - n_{eqv}}{-R_p}, \tag{23}$$

where the equivalent refractive index n_{eqv} provides the equivalent optical power for the lens. Equating the right hand sides of Eqs. (22) and (23) and solving for n_{eqv} result

$$n_{eqv} = \frac{2p\,n_c - n_s}{2p - 1}. \tag{24}$$

The definition of n_{eqv} by Eq. (24) is not limited to the main wavelength and can be expanded to the equivalent powers of other wavelengths as

$$n_{eqv}(\lambda) = \frac{2p(\lambda)\,n_{center}(\lambda) - n_{surface}(\lambda)}{2p(\lambda) - 1}. \tag{25}$$

Substituting Eq. (24) in Eq. (12) leads to the equivalent Abbe number of the equivalent lens. If the change in p with wavelength λ is negligible the equivalent Abbe number can be rewritten as

$$V_{eqv}(\lambda) = \frac{V_{dc}V_{ds}\left[n_s - 1 - 2p\,(n_c - 1)\right]}{V_{dc}\,(n_s - 1) - 2p\,V_{ds}\,(n_c - 1)}, \tag{26}$$

where V_{dc} and V_{ds} are the Abbe numbers of the center and the surface of the GRIN lens, respectively. As an example, Table 1 presents the calculated lens equivalent refractive index n_{eqv} and the equivalent Abbe number V_{eqv} using the dispersion data from Sivak and Mandelman [11], and Palmer and Sivak [10] for $p = 3.0$ (representing a 34-year old eye according to the study by Navarro *et al.* [8]).

Employing the equivalent refractive indices and Abbe numbers listed in Table 6, one can calculate the axial and lateral color coefficients of the equivalent lens. These coefficients are approximate, while the exact color coefficients derived in Eqs. (18) and (20). The comparison between the axial and lateral color of a typical GRIN lens and its equivalent refractive index lens is presented in Table 7. Here, the angles and the height of the incident rays, and the geometry

Table 6. The calculated quantities n_{eqv} and V_{eqv} using the dispersion data from Sivak and Mandelman [11], and Palmer and Sivak [10] for a typical $p = 3.0$.

Data set	n_c	n_s	n_{eqv}	V_{dc}	V_{ds}	V_{eqv}
Sivak and Mandelman	1.4018	1.3751	1.4071	33.71	27.23	35.25
Palmer and Sivak	1.3968	1.3750	1.4011	42.73	81.95	39.22

Table 7. A comparison between the exact and equivalent color coefficients calculated respectively for a typical GRIN lens and its equivalent refractive index lens.

Data set	Equivalent $\sum C_L$	Exact $\sum C_L$	Equivalent $\sum C_T$	Exact $\sum C_T$
Sivak and Mandelman	-0.000856	-0.000852	-0.000034	-0.000035
Palmer and Sivak	-0.000618	-0.000626	-0.000024	-0.000022

of the lens and its surrounding media are the same as in the previous numerical examples (See Section 3.2.1), except for the exponent p, here $p = 3.0$.

Table 7 demonstrate a good agreement between the exact and equivalent color coefficients, which indicates practical advantages of this approach in finding the exact equivalent optical characteristics. However, replacing a complicated GRIN structure with a homogeneous material will not transfer all optical characteristics of the lens simultaneously. Here, the equivalent refractive index calculation aims at preserving the optical power of the lens, yet other optical characteristics of the lens need their own equivalent refractive index. As an example, we consider the optical path length (OPL) in the GRIN lens. The axial OPL in GIGL [3] is derived as

$$OPL = (T_a + T_p)\frac{2n_c p + n_s}{2p + 1}, \tag{27}$$

which defines the quantity $(2n_c p + n_s)/(2p + 1)$ as the equivalent refractive index in the OPL calculation of the lens. This OPL equivalent refractive index known as the average refractive index [19] is different from the one calculated in Eq. (24).

5. Axial Chromatic aberration and aging

There are two independent studies, which found no significant changes in the magnitude of chromatic aberration with age [20, 21], but some earlier studies claim that the magnitude of chromatic aberration decreases with age [22, 23]. Considering the growth of the GRIN lens, it is well known that for an unaccommodated lens, the external surfaces become more curved with aging [24]. The lens considered in Section 3.2.2 shows positive axial color coefficients at its surfaces (Table 4). Aging lens increases the optical power of its surfaces, thus this lens surfaces will show larger positive axial color coefficients, see Eq. (11). In addition to this, the chromatic effect arising from the GRIN structure should be taken into account. To examine the role of the GRIN structure in the age-related chromatic effect individually, we keep the geometry of the lens in Section 3.2.2 unchanged, only adjust the age-related exponent p to three different age groups. Following the study by Navarro et al. [8] we selected three age groups (20, 40, and 60 year old) with corresponding value for p and calculated the resultant axial color coefficients for each group in Table 8.

Table 8 indicates that the magnitude of the axial color coefficient originated from the GRIN structure of the lens decreases due to an increase in the exponent p. Looking at the sign of the coefficients of the lens surfaces, it is evident that the total axial color coefficient of the lens goes toward zero or even positive amounts. As mentioned in Section 3.2.1, a typical cornea

Table 8. The axial color coefficients from the GRIN structure for three age groups (20, 40, and 60 year old) using the dispersion data provided by Palmer and Sivak [10].

Age (year)	p	C_L from the GRIN structure
20	2.87	-0.001046
40	3.13	-0.001028
60	4.28	-0.000977

shows a negative axial color coefficient. Due to aging, the surfaces of the cornea get slightly more curved [25], which increases the magnitude of this negative corneal axial color coefficient. Considering these two effects for the GRIN lens and the cornea, one could argue that the eye, as a whole, might show a constant or a better chromatic performance with aging.

It is worth mentioning that employing the Sivak and Mandelman's data in the same approach provides an increase in the total axial color coefficient, which does not support the argument above. Since the dispersion data from Sivak and Mandelman is averaged over 6 to 9 subjects with different ages, some valuable information of each individual lens might be missing. This highlights the need of more chromatic measurements on the GRIN lens and its surrounding media for a more confident conclusion.

6. Discussion and conclusion

In this study the potential of the existing GIGL monochromatic model [3] has been realized and demonstrated by introducing a flexible chromatic GRIN lens model. The model is examined with different data fittings to gain better understanding of the GRIN lens chromatic aberration behavior of the lens. The advantages of the provided equations are not limited to this data fitting only, since the model can also be used to help explaining other chromatic characteristics of the eye for example spherochromatism. The latter can be calculated using the spherical aberration coefficients for different color wavelength.

We would like to emphasize that the provided model should be regarded as a tool, which can be employed in experimental data fitting and further analysis for better understanding of the chromatic nature of the eye. The scope of the chromatic model is not limited to the human eye and can be applied to animal GRIN lenses, where unusual chromatic behavior might happen (*e.g.* [26, 27]). Table 9 provides the axial color coefficients of a semi-spherical octopus eye lens calculated based on the measurements from Jagger and Sands [27].

Table 9. The chromatic coefficients of a typical octopus GRIN lens using the dispersion data from Jagger and Sands [27].

Axial color coefficients	
C_L from the anterior surface	-0.000779
C_L from the GRIN structure	-0.003499
C_L from the posterior surface	-0.000629
ΣC_L	-0.004909

The proposed dispersive GIGL model completes the description of the monochromatic GIGL model. The concept of iso-dispersive contours introduced in this paper is a unique feature of the dispersive GIGL model. The optically-friendly geometry of the GIGL model featuring iso-dispersive contours (constant Abbe number V_d) supports the calculations for the contribution of the individual layers to the total chromatic effects of the lens. Thus the model gives a new insight in the derivation of the equivalent Abbe number based on experimental dispersion curves

for the center and the surface of the lens. The proposed model offers easy analysis of equivalent refractive index and OPL equivalent index. One could use the model to investigate chromatic aberration evolution in the aging human eye, in particular the effect of the power constant p on the color coefficients. The model also predicts the amount of induced defocus (change in optical power with wavelength) when using different wavelengths, *e.g.* adaptive optic system with wavefront sensor operating at one wavelength and the retinal imaging at another wavelength, although retinal absorption effects still have to be included in this case.

Acknowledgments